In: ANTEC® 2017 - Proceedings of the Technical Conference & Exhibition, Anaheim, California, USA May 8-10, 2017. Society of Plastics Engineers, 2017, EISBN: 978-1-5231-1668-3

INFLUENCE OF THE FIBER-MATRIX-INTERACTION ON THE FRACTURE BEHAVIOR OF REGENERATED CELLULOSE FIBER REINFORCED POLYPROPYLENE

Jan-Christoph Zarges, Christian Kaufhold, Maik Feldmann, Hans-Peter Heim*
Institute of Material Engineering, Polymer Engineering, University of Kassel, Germany

Abstract

This investigation focuses on the fiber-matrix-interaction of man-made cellulose fibers (RCF) in a PP matrix with an additional MAPP content using an energetic evaluation of the single fiber pull-out test (SFPT). Furthermore glass fibers were characterized for reference purposes. With the SFPT the interfacial shear strength (IFFS) and the critical fiber length (lc) as well as the consumed energy of a fiber pull-out and a fiber rupture were determined. In a following step the resulting values of l_c were related to the fiber length distribution in injection molded specimens. It was shown that, based on the longer RCF in the specimen, theoretically more fiber ruptures appear in the RCF composites. But the RCF composites also contain a higher number of long fibers, consuming a higher amount of energy by being pulled out during a composite failure. The length-dependent consumed energy of a fiber pull-out was increased by using MAPP but simultaneously the critical fiber length was significantly reduced.

Introduction

With a wider range of applications of natural fiber composites (NFC), e.g. in the automobile industry, during the last decade the characterization of those composites gets in the focus of research as well [1–3]. In previous studies cellulosic fibers, such as wood pulp or regenerated cellulose fibers (RCF), have been used as reinforcement and the resulting composites showed tensile strengths comparable with glass fiber (GF) reinforced composites and especially significantly higher notched impact strength and fracture toughness [4-8]. Next to the advantages in the mechanical properties, the use of cellulosic fibers offers significant potential regarding lightweight applications, based on their lower density compared to a conventional glass fiber reinforcement [3,9,10].

Regarding the mechanical properties of fiber reinforced composites it is well known, that the fiber-matrix-interaction has a significant influence. If the occurring load in the reinforcement fiber exceeds their tensile strength, fiber-rupture will occur, that results in the optimal reinforcing effect. To achieve this effect, fibers have to be longer than the critical fiber length, which is a specific value for each fiber-matrix-system. If the fibers are shorter than the critical fiber length, they will not rupture but pulled out of the matrix.

In this context the higher notched impact strength [7,13] and fracture toughness [11,15] of regenerated cellulose fibers reinforced PP was attributed to a high number of fiber pull-outs due to a weak interface and the friction occurring during this process [4,8]. In turn, an improvement of the fiber-matrix adhesion leads to less pull-outs and at least to reduced values of the impact strength and fracture toughness [12-14]. Although the high fracture toughness and notched impact strength can be well attributed to long friction involving fiber pull-outs, it was not proofed that a fiber pull-out is indeed more energy consuming than a fiber rupture.

In this investigation, the fiber-matrix adhesion of regenerated cellulose fibers and a PP matrix, described with the values of the interfacial shear strength (IFFS) and the critical fiber length (l_c), was characterized by means of frequently used single fiber pull-out test (SFPT) [16-20]. Furthermore the influence of the coupling agent MAPP and the process induced thermal impact on the fibers was evaluated and compared to glass fibers, which were used for reference purposes. The critical fiber length was set in relation to the present fiber length distribution in injection molded specimens to evaluate a theoretical amount of ruptured and pulled-out fibers. Moreover, the occurring energy of a fiber pull-out and a fiber rupture was determined and compared to justify its influence on the mechanical properties.

Materials

The Polypropylene 575P used as matrix polymer was provided by Sabic. To determine the influence of a coupling agent, a PP matrix with a content of 4.3 wt.% MAPP, provided by Clariant, was also characterized. This content was chosen because it complies with the previously investigated content of 3 wt.% after adding 30 wt.% fibers for the injection molded composites. The fibers used for embedding are endless regenerated cellulose fibers CR-type, provided by Cordenka, with a filament diameter of approx. 12 µm. Furthermore, endless E-glass fibers with a fiber diameter of approx. 12 µm and a silane-based sizing, provided by R&G Composite Technology, were used.

To set the values of the critical fiber length in relation to the fiber length distribution in injection molded specimen, chopped CR-fibers with a length of 2.3 mm as well as glass fibers CS 7952 with an average fiber length of 4.5 mm and a diameter of 14 µm, provided by Lanxess, were used for composites preparation. The fiber content was set to 30 wt.%.

Film Manufacturing

To prepare the samples for the SFPT, the fibers were embedded between films of the matrix material, which is

melted in a second step. The films were manufactured using a single screw extruder (Gimac) with a slit die and a downstream calender, provided by Dr. Collin. The resulting thickness of the PP-films was 120 µm and 80 µm of those with a content of 4.3 wt.% MAPP.

Fiber Conditioning

The influence of the necessary drying process and the thermal loads of the compounding and injection molding process on the fiber-matrix adhesion was determined by conditioning the fibers prior to the sample preparation (see Table 1). As a reference, fibers in an unconditioned state were tested.

Table 1. Conditioning states and parameters

Conditioning state	**1**	**2**
Conditioning Parameter	unconditioned	105°C / 24h + 210°C / 5min

Specimen Preparation

To determine the interfacial shear strength and the critical fiber length by using the single fiber pull-out test, the fibers had to be embedded in the matrix material. To realize that, two fibers per specimen were positioned between the film sheets which were subsequently melted under defined conditions. Therefore a mold in a hot press, provided by Ott, was used. The pressure in the mold was set to 2 N/mm² and the temperature to 190 °C. At the end of the pressing process the specimen were cooled down at ambient air temperature. In a second step, strips from the edge region with the sticking out fibers were cut off with a precision scissor (see Figure 1).

To enable a pull-out, the height of the strips, representing the embedded fiber length, was needed to be smaller than the critical fiber length. For that reason the strips were prepared with a height of 250-450 µm for the cellulose fibers and 250-800 µm for glass fibers.

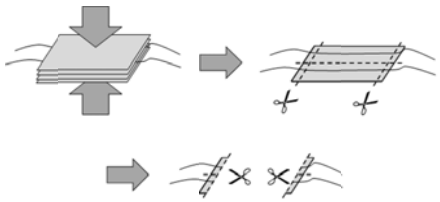

Figure 1: Scheme of the sample preparation for the SFPT

Injection Molding

To set the critical fiber length in relation to the fiber length distribution in injection molded specimen, plates with a size of 72 x 72 x 10 mm were manufactured with an injection molding machine. These plates were already used to prepare CT-specimen for the evaluation of the fracture toughness in former investigations [11].

Characterization

All specimens were characterized in a standardized climate (23°C, 50% relative humidity).

Single Fiber Tensile Test

Prior to the characterization of the fiber-matrix adhesion with the SFPT, the tensile properties of the single fiber were investigated. Therefore single fiber tensile tests were carried out with a speed of 5 mm/min using the single fiber testing machine Favimat+, provided by Textechno. A clamping lengths of 0.5 was used.to realize the same free fiber length used in the SFPT. The free fiber length is the length of the fiber from the top of the embedding film and the bottom of the upper clamp, in which the free end of the fiber is fixed (see Figure 2). All fibers were tested in an unconditioned and a conditioned state, according to Table 1.

The perimeter (p_f) and the cross sectional area of the fibers have been evaluated with a digital microscope (Keyence VHX-600) and the open source software ImageJ. For that measurement several fibers were fixed in a cold-setting epoxy resin type Araldite DBF BD, provided by the company Huntsman.

Single Fiber Pull-Out Test

The SFPT was carried out at a speed of 5 mm/min and a free fiber length of 0.5 mm using the Favimat+ (see Figure 2). Due to the soft rubber material of one clamping jaw the deformation of the specimen was reduced to a minimum. Furthermore, that soft material allows extremely low clamping forces because of to a static friction. As the lower clamp moved down the fiber was pulled out of the matrix and the load-displacement curves were recorded.

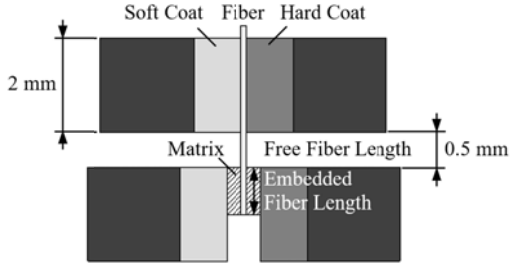

Figure 2: Clamping setup of the SFPT with the Favimat+

After the pull-out occurred, the length of the empty fiber channel was measured with the described digital microscope to evaluate the embedded fiber length (l_{ef}). According to Kelly and Tyson [21] the apparent interfacial shear strength (IFSS) τ can be calculated with the value of l_{ef} and the perimeter of the fiber (p_f) using equation (1).

$$\tau = \frac{F_{max}}{d_f \cdot \pi \cdot l_{ef}} = \frac{F_{max}}{p_f \cdot l_{ef}} \qquad (1)$$

The resulting critical fiber length l_c was determined with the calculated τ and the tensile strength σ_f of the fiber according to equation (2).

$$l_c = \frac{\sigma_f \cdot d_f}{2 \cdot \tau} \qquad (2)$$

Dynamic Image Analysis

To measure the fiber length distribution in the injection molded specimens the dynamic image analysis system QICPIC, provided by Sympatech, was applied. For this analysis, a small piece of the specimen was cut out and the matrix of the composites was subsequently dissolved by boiling xylene. The system took images of the passing fibers and the length distribution of 10.000 measured fibers was evaluated by the software Windox afterwards.

Results and Discussion

Fiber Properties

The mechanical properties of the reinforcement fibers were evaluated in single fiber tensile tests at 5 mm/min using the Favimat+ with a clamping length of 0.5 mm and are shown in Table 2.

Table 2. Properties the reinforcement fibers.

	RCF		GF	
Density [g/cm³]	1,5		2,6	
Conditioning state	1	2	1	2
Fiber tensile strength [MPa]	900 ±72	1040 ±51	2960 ±444	2900 ±448
Elongation at break [%]	18,42 ±1,57	13,22 ±1,66	3,42 ±0,67	3,49 ±0,73
Diameter [µm]	12,65 ±0,28	12,62 ±0,26	12,64 ±0,61	12,71 ±0,6)
Perimeter [µm]	47,13 ±3,80	46,96 ±1,22	39,74 ±3,03	39,94 ±1,88

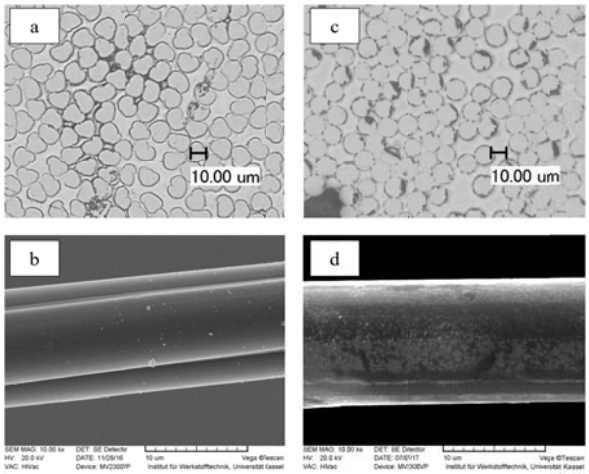

Figure 3: Cross section and SEM pictures of RCF (a,b) and GF(c,d)

The perimeter and the cross sectional area determined with the microscopic images shown in Figure 3 (a, b) and the results are shown in Table 2. These figures and also the SEM pictures (c, d) show the form of the RCF which deviates from the circular shape of the GF. Furthermore the SEM images constitute the rougher surface of the GF which can be explained by the silane-based sizing.

Evaluation of the SFPT

The apparent IFFS was calculated by dividing the maximum load of a fiber pull-out by the outside surface of the fiber, which is in contact with the matrix, according to equation (1). Figure 4 shows typical load-displacement curves of fiber pull-outs as well as fiber ruptures during the SFPT.

During the SFPT, the load increases up to a maximum value, at which the fiber separates from the matrix due to a failure of the interface. In case of the neat PP, the load slightly decreases afterwards, while a long friction involving pull-out of the fiber occurs (Figure 4). In comparison to that, the MAPP containing matrices reach a higher maximum load before a sharp drop of the load due to the failure of the interface occurs.

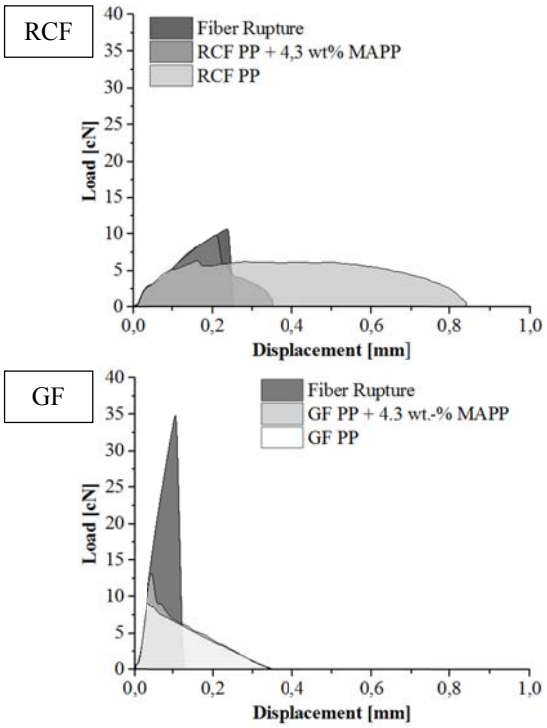

Figure 4: Load-displacement curves of fiber pull-out and rupture

The calculated apparent IFFS of the two conditioning states is depicted in Figure 5a and shows rising values with the added coupling agent for all fibers and fiber conditions. An addition of 4.3 wt.% MAPP leads to an increase of the interfacial shear strength of approx. 77 % in case of the RCF and 57 % in case of the GF (both

conditioning state 2). Furthermore the increase of 12% due to a conditioning of the RCF in neat PP was also remarkable. These results lead to the conclusion that the thermal load of the processing improves the fiber-matrix adhesion of the RCF. In contrast to that, the IFSS of the thermally more stable GF is only minor affected by the conditioning.

Compared to the RCF the GF shows higher values of apparent IFSS in all used matrix materials which can be explained with a rougher and more heterogeneous surface caused by the sizing (see Figure 3). This silane-based sizing was applied by the manufacturer to improve the bonding to the matrix material. Due to the interaction of this sizing and the functional groups of the MAPP, the IFSS of the GF also increases with the addition of the coupling agent.

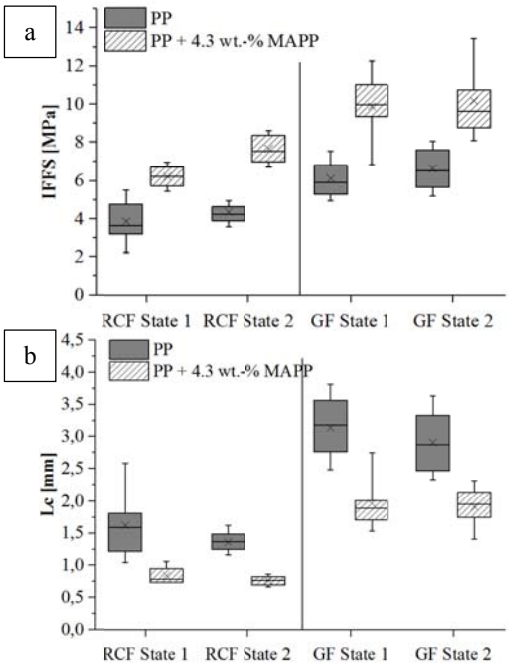

Figure 5: Apparent interfacial shear strength (a) and critical fiber length (b) of RCF and GF

According to equation (2), the apparent critical fiber length was calculated based on the apparent IFSS, the fiber tensile strength and the fiber diameter (Figure 5a).

Based on the increase of the apparent IFSS, the apparent critical fiber length is reduced due to the added coupling agent (Figure 5b). The apparent critical fiber length of RCF in conditioning state 1 is reduced from 1.61 mm in neat PP to 0.94 mm and in a PP with 4.3 wt.% MAPP from 1.35 mm to 0.75 mm in conditioning state 2. Thus, the apparent critical fiber length is reduced by more than 40% due to an addition of 4.3 wt.% MAPP whereas the conditioning leads to a reduction of about 18 %. For the GF, the decrease caused by the MAPP is about 38% whereas the conditioning of GF only caused minor deviations. Although the GF show higher values of the apparent IFSS than the RCF, the apparent critical fiber length is considerable higher. This can be justified with a significant higher tensile strength of the GF (see Table 2).

To compare the evaluated critical fiber length with the fiber length distribution in injection molded specimen, the length of each fiber, measured with the dynamic image analyzing system, was set in relation to the mean value of the determined apparent critical fiber length (see Figure 6).

The results of the fiber length distribution in Figure 7 reveal that RCF are shortened as well, but due to their lower bending stiffness, processing has less impact on them. In comparison to GF the length distribution of the RCF offers a higher number of long fibers, which are supposed to have an impact on the composites tensile strength.

With the resulting fiber length distribution and the values of l_c a ratio of the amount of fibers with a length higher or lower than the critical fiber length was determined. As a result of this calculation only 4% of the RCF in a composite with neat PP and 16% in a composite with PP and 4.3 wt.% MAPP showed length higher than the critical fiber length and, in turn, rupture due to the exceeded fiber tensile strength. In comparison to that less than 0.1% of all GF rupture. Because of these similar results, the deviating properties of GF and RCF reinforced composites e.g. the fracture toughness cannot only be explained by the ratio of fiber fracture and pull-out [11]. In fact, the energy consumption of both occurrences must be considered and are explained in the following.

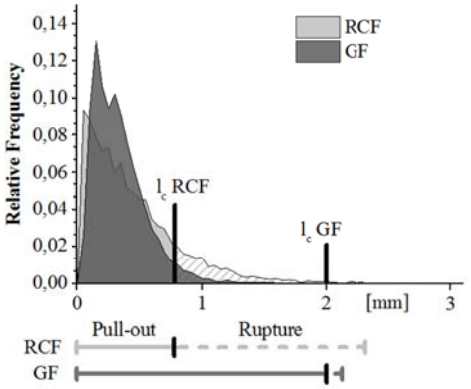

Figure 6: Critical fiber length in relation to the fiber length distribution RCF and GF

Energetic Evaluation of the SFPT

The energy consumption of the fiber pull-out results from the area under the load displacement curve (see Figure 4) and depends on the embedded fiber length. With an increasing embedding length the pull-out length as well as the maximum load and, in turn, the consumed energy increases (Figure 7). The addition of the coupling agent also results in a higher work necessary to separate the fiber from the matrix. After this separation the process

of the pull-out itself takes place at comparable energy levels (see figure 4).

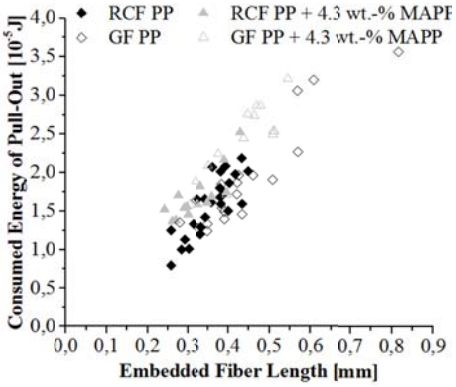

Figure 7: Consumed energy of a fiber pull-out over embedded fiber length

To determine the minimal embedded fiber length above which a fiber pull-out consumes more energy than a fiber rupture, the energy consumption of a rupture was evaluated. Therefore, the SFPT was carried out with embedded fiber lengths well above the apparent critical fiber length. This was done at different free fiber lengths and the resulting values were extrapolated to a length of zero because there is no free fiber length expected in the composites. The mean value of the energy consumption of a fiber rupture was found to be independent of the matrix material and was determined to be approx. $0.763 \cdot 10^{-5}$ J for the RCF and $1.86 \cdot 10^{-5}$ J for the GF.

Figure 8 shows the frequency of ruptured and pulled out fibers with lower and higher energy consumption than a fiber rupture. Furthermore, the work at which a fiber pull-out starts to be more energy consuming than a rupture as well as the maximum work of a fiber pull-out is depicted.

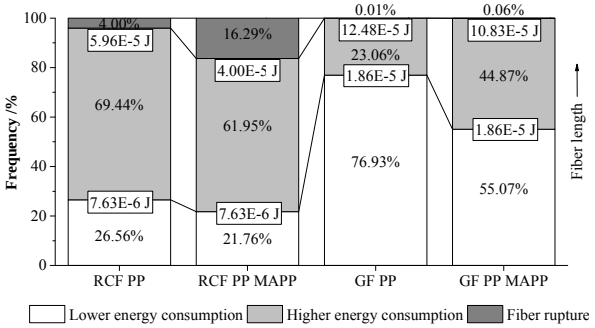

Figure 8: Frequency of fiber pull-out and fiber rupture in injection molded specimens

Due to the reduction of the critical fiber length by adding the MAPP, there were obviously more ruptured RCF and, in turn, a reduced number of fiber pull-outs. Although the MAPP leads to a higher energy consumption at comparable embedded fiber lengths, the fiber pull-outs consuming the maximum energy occur in neat PP by means of higher possible pull-out lengths. Here, the maximum energy consumption was approx. $5.96 \cdot 10^{-5}$ J at a pull-out length of 1.35 mm and in PP with 4.3 wt.% MAPP it was approx. $4 \cdot 10^{-5}$ J at 0.75 mm length.

The consumed energy of a fiber pull-out matched the energy of a fiber rupture at an embedded fiber length of 0.17 mm (0.43 mm for GF) in neat PP and 0.15 mm (0.32 mm for GF) in the MAPP containing matrix. This means that fibers with an embedded length shorter than this value consumed less energy than longer fibers that rupture. With values of $12.48 \cdot 10^{-5}$ J for neat PP and $10.83 \cdot 10^{-5}$ J for PP with 4.3 wt.% MAPP the maximum consumed energy of the GF pull-out was significantly higher than a pull-out of the RCF. This is caused by the longer apparent critical fiber length of GF and, in turn, a theoretically higher possible pull-out length. But in fact, there is only a small amount of less than 2% of the GF near the apparent critical fiber length leading to this significant higher work. Due to the fact that almost all GF in injection molded specimens were well underneath the apparent critical fiber length, the coupling agent did not significantly increase the amount of fiber ruptures, in contrast to the RCF.

Conclusions

The SFPT was used to evaluate the fiber-matrix adhesion between PP and RCF considering GF for reference purposes. The evaluation of the fiber-matrix adhesion was carried out taking the apparent IFSS and the apparent critical fiber length into account. Thereby the influence of the coupling agent MAPP and two conditioning states of the fibers was investigated.

The results of the SFPT revealed that the fiber-matrix adhesion can be improved by adding the coupling agent, both for RCF and GF. In addition to that, the fiber-matrix adhesion of RCF was improved by conditioning.

A comparison of the calculated apparent critical fiber length with the fiber length distribution in injection molded specimens led to the result that almost all present GF are shorter than the critical fiber length so that, in turn, no fiber rupture in the GF composites will appear. In contrast to that about 4% of the RCF in a PP matrix exceed the apparent critical fiber length and were able to obtain a maximum reinforcing effect. By adding 4.3 wt.% MAPP to the PP matrix, the percentage of fiber ruptures is raised to 16%. Furthermore, it was shown that a fiber pull-out is only more energy consuming than a rupture above a specific embedded length.

The percentage of fiber pull-outs was found to be lower in RCF composites than in GF composites, but the RCF offer longer fibers in injection molded specimens and therefore longer and more energy consuming fiber pull-outs. Due to that fact, not the amount but the higher consumed energy of the pulled-out RCF is a criterion of a high impact strength and fracture toughness.

For all fibers, the work of fiber pull-outs was increased by adding MAPP, but simultaneously the apparent critical fiber length was reduced. That results in less and shorter fiber pull-outs in case of RCF composites and a related decrease of the consumed energy whereas the amount and length of pull-outs in GF composites was not affected by the coupling agent.

Although the composite properties do not only depend on fiber-matrix interactions, but also on the fiber volume content, aspect ratio of fibers and fiber orientations etc., the presented results provide a good explanation for the composites properties shown in other publications.

References

1. Furtado, S. C., Araújo, A. L., Silva, A., Alves, C. & Ribeiro, A. (2014). Natural fibre-reinforced composite parts for automotive applications. International Journal of Automotive Composites, 1(1), 18–38.
2. Holbery, J. & Houston, D. (2006). Natural-fiber-reinforced polymer composites in automotive applications. JOM, 58(11), 80–86.
3. Njuguna, J., Wambua, P., Pielichowski, K. & Kayvantash, K. (2011). Natural fibre-reinforced polymer composites and nanocomposites for automotive applications. In: Kalia, S., Kaith, B.S., Kaur, I. (editors). Cellulose Fibers: Bio- and Nano-Polymer Composites. Berlin, Heidelberg: Springer; p. 661–700.
4. Zarges, J.-C., Feldmann, M. & Heim, H.-P. (2014). Influence of the compounding process on bio-based polyamides with cellulosic fibers. In: 30th International conference of the Polymer Processing Society, Cleveland, Ohio, USA.
5. Feldmann, M. (2016). The effects of the injection moulding temperature on the mechanical properties and morphology of polypropylene man-made cellulose fibre composites. Composites Part A, 87, 146–152.
6. Ganster, J., Fink, H.-P., Uihlein, K. & Zimmerer, B. (2008). Cellulose man-made fibre reinforced polypropylene-correlations between fibre and composite properties. Cellulose, 15(4), 561–569.
7. Bledzki, A. K. & Jaszkiewicz, A. (2010). Mechanical performance of biocomposites based on PLA and PHBV reinforced with natural fibres – a comparative study to PP. Composites Science and Technology, 70(12), 1687–1696.
8. Feldmann, M. & Bledzki, A. K. (2014). Bio-based polyamides reinforced with cellulosic fibres – Processing and properties. Composites Science and Technology, 100, 113–120.
9. Fernandez, J. L. R. & Thomason, J. (2012). Characterisation of the mechanical performance of natural fibres for lightweight automotive applications. In: 15th European conference on composite materials, p. 1231.
10. Pandey, J. K., Ahn, S. H., Lee, C. S., Mohanty, A. K. & Misra, M. (2010). Recent advances in the application of natural fiber based composites. Macromolecular Materials and Engineering, 295(11), 975–989.
11. Zarges, J. C., Minkley, D., Feldmann, M. & Heim, H. P. (2017). Fracture toughness of injection molded, man-made cellulose fiber reinforced polypropylene. Composites Part A, 98, 147–158.
12. El-Sabbagh, A. (2014). Effect of coupling agent on natural fibre in natural fibre/polypropylene composites on mechanical and thermal behaviour. Composites Part B, 57, 126–135.
13. Ganster, J. & Fink, H.-P. (2006). Novel cellulose fibre reinforced thermoplastic materials. Cellulose, 13(3), 271–280.
14. Ganster, J., Fink, H.-P. & Pinnow, M. (2006). High-tenacity man-made cellulose fibre reinforced thermoplastics – injection moulding compounds with polypropylene and alternative matrices. Composites Part A, 37(10), 1796–1804.
15. Zarges, J.-C., Feldmann, M., Heim, H.-P., Judt, P. & Ricoeur, A. (2017). Man-made cellulose fiber reinforced polypropylene – characterization of fracture toughness and crack path simulation. In ANTEC Proceedings. Anaheim, CA, USA.
16. Graupner, N., Rößler, J., Ziegmann, G. & Müssig, J. (2014). Fibre/matrix adhesion of cellulose fibres in PLA, PP and MAPP: a critical review of pull-out test, microbond test and single fibre fragmentation test results. Composites Part A, 63, 133-48.
17. Adusumalli, R.-B., Reifferscheid, M., Weber, H. K., Roeder, T., Sixta, H. & Gindl, W. (2012). Shear strength of the lyocell fiber/polymer matrix interface evaluated with the microbond technique. Journal of Composite Materials, 46(3), 359–367.
18. Yang, L. & Thomason, J. L. (2012) Development and application of micromechanical techniques for characterising interfacial shear strength in fibrethermoplastic composites. Polymer Testing, 31(7), 895–903.
19. Nirmal, U., Singh, N., Hashim, J., Lau, S. T. & Jamil, N. (2011). On the effect of different polymer matrix and fibre treatment on single fibre pullout test using betelnut fibres. Materials & Design, 32(5), 2717–2726.
20. Jia, Y., Yan, W. & Liu, H.-Y. (2012). Carbon fibre pullout under the influence of residual thermal stresses in polymer matrix composites. Computational Materials Science, 62, 79–86.
21. A. Kelly & W.R. Tyson. (1965). Tensile properties of fibre-reinforced metals: Copper/tungsten and copper/molybdenum. Journal of the Mechanics and Physics of Solids, 13(6), 329–350.